Nucleation and Growth of Lead Sulfide Nano- and Microcrystallites in Supramolecular Polymer Assemblies

Ashim K. Dutta, Thaotrang Ho, Liqin Zhang, and Pieter Stroeve*

Center on Polymer Interfaces and Macromolecular Assemblies (CPIMA), Department of Chemical Engineering and Materials Science, University of California−Davis, Davis, California 95616

Received October 8, 1999. Revised Manuscript Received January 12, 2000

Multilayer thin film assemblies fabricated by the sequential adsorption of polyelectrolytes on a quartz substrate were used as a supramolecular reaction template to study the in situ nucleation and growth of PbS nano- and microparticles. Chemical reaction within the polymer film was initiated by absorbing Pb^{2+} from an aqueous solution of $Pb(NO_3)_2$ followed by exposing the film to H_2S gas. Electron microscopic examination of the films revealed that while nanoparticles are formed in films that were subject to one or two reaction cycles, large crystallites were formed when these films were exposed to a large number (10) of reaction cycles. In the latter case, a broad distribution of particle sizes is observed and may be attributed to Ostwald ripening. Detailed studies show the nucleation and growth of the PbS particles into crystallites of different shapes. UV−vis absorption studies reveal that the absorption spectral profiles of the films are dependent on the size of the PbS crystallites. The broadened absorption spectral profile observed for films subject to a large number of reaction cycles may be attributed to the superposition of the spectral profiles of the small clusters that tend to be blueshifted due to quantum confinement effects and the large clusters that are redshifted.

Introduction

In recent years, the fabrication of nanostructured materials and exploration of their properties have attracted the attention of physicists, chemists, biologists, and technologists alike.[1] Interest in such systems arise from the fact that the mechanical, chemical, electrical, optical, magnetic, and electro- and magneto-optical properties of these particles are different from their bulk properties and depend on the particle size.[2] These nanoparticulate systems are deemed technologically important in the design of miniaturized, ultrahigh-density integrated circuits and information storage devices of the future and in some sense an alternate route to overcome the 100 nm barrier in conventional electronics and develop nanodimensional molecular electronic devices.[3]

Because of their semiconducting properties, group II−VI and IV−VI compounds have been intensively examined by various authors.[4] The size-dependent optoelectronic properties of nanoparticles (diameter 1−100 nm) is attributed to quantum confinement effects.[1−3] Briefly, electronic excitation in semiconductors arise from an exciton (an electron and hole bound pair) localized in a potential well. Theoretical calculations[2,3] have demonstrated that when particle sizes corresponding to the de Broglie wavelength of the free charge carriers are approached, quantum confinement effects become dominant.[2,3] One manifestation of such an effect is an increase in the optical band gap energy with decreasing particle size that is readily manifested as sharp changes in color visible to the naked eye. On the basis of particle size, the color of CdS colloids may vary from blue to red while PbS nanoparticles may appear pale yellow, orange, red, or black.

Nanoparticles has been studied in micelles,[5] vesicles,[6] sol−gel glasses,[7] zeolites,[8] Langmuir−Blodgett (LB) films,[9] and polymers.[10] In most cases, the clusters have poorly defined surfaces and a broad distribution of

* Telephone: (530) 752-8778. Fax: (530) 752-1031. E-mail: pstroeve@ucdavis.edu.

(1) (a) Nirmal, M.; Brus, L. *Acc. Chem. Res.* **1999**, *32*, 407. (b) Alivisatos, A. P. *Science* **1996**, 271, 933. (c) Chan, W. C. W.; Nie, S. *Science* **1998**, *281*, 2016. (d) Bruchez, M.; Moronne, M.; Gin, P.; Weiss, S.; Alivisatos, A. P. *Science* **1998**, *281*, 2013.

(2) (a) Brus, L. E. *Appl. Phys. A* **1991**, *53*, 465. (b) Brus, L. E. *J. Chem. Phys.* **1984**, *80*, 4403. (c) Wang, Y. *Acc. Chem. Res.* **1991**, *24*, 133. (d) Henglein, A. *Topics Curr. Chem.* **1988**, *143*, 113. (e) Steigerwald, M. L.; Brus, L. E. *Acc. Chem. Res.* **1990**, *23*, 183. (f) Brus, L. E. *Springer Ser. Chem. Phys.* **1994**, *56*, 312. (g) Weller, H. *Angew. Chem., Intl. Ed. Engl.* **1993**, *32*, 41. (h) Weller, H. *Adv. Mater.* **1993**, *5*, 88. (i) Henglein, A. *Chem. Rev.* **1989**, *89*, 1861.

(3) (a) Koyama, H.; Araki, M.; Yamamoto, Y.; Koshida, N. *Jpn. J. Appl. Phys.* **1991**, *30*, 3606. (b) Dabbousi, B. O.; Bawendi, M. G.; Onitsuka, O.; Rubner, M. F. *Appl. Phys. Lett.* **1995**, *66*, 1316. (c) Nirmal, M.; Dabbousi, B. O.; Bawendi, M. G.; Macklin, J. J.; Trautman, J. K.; Harris, T. D.; Brus, L. E. *Nature* **1996**, *383*, 802. (d) Cassagneau, T.; Mallouk, T. E.; Fendler, J. H. *J. Am. Chem. Soc.* **1998**, *120*, 7848. (e) Brus, L. E. *J. Phys. Chem.* **1994**, *98*, 3575.

(4) (a) *Semiconductor Nanoclusters−Physical, Chemical and Catalytic Aspects*; Kamat, P. V., Meisel, D., Eds.; Elsevier: Amsterdam, 1997. (b) Kortan, A. R.; Hull, R.; Opila, R. L.; Bawendi, M. G.; Steigerwald, M. L.; Caroll, R. J.; Brus, L. E. *J. Am. Chem. Soc.* **1990**, *112*, 1327. (c) Hoener, C. F.; Allan, K. A.; Bard, A. J.; Campion, A.; Fox, M. A.; Mallouk, T. E.; Webber, S. E.; White, J. M. *J. Phys. Chem.* **1992**, *96*, 3812. (d) Zhou, H. S.; Sasahara, H.; Honma, I.; Komiyama, H. *Chem. Mater.* **1994**, *6*, 1534. (e) Hasselbarth, A.; Eychmuller, A.; Weller, H. *J. Phys. Chem.* **1993**, *97*, 5333. (f) Schoos, D.; Mews, A.; Eychmuller, A.; Weller, H. *Phys. Rev. B* **1994**, *49*, 17072.

10.1021/cm990628c CCC: $19.00
Published on Web 03/14/2000

particle sizes. Bawendi and co-workers[11] have demonstrated control in preparing monodisperse CdSe clusters using a synthesis medium consisting of trioctylphosphine and its oxide. While size exclusion chromatography permits a narrow size distribution of particle sizes, only minute quantities of the materials are obtained which is unsuitable for any large-scale applications. On the contrary, the synthetic route used by Bawendi et al.[11] permits the production of gram quantities of nanoparticulate solids that may again be methathesized with surface agents to produce clusters soluble in an variety of solvents providing access to different processing opportunities. Chemical reactions initiated within the microscopic cavities of zeolites, glasses, and micelles provide an easy and elegant process of preparing nanoparticles. The shape and sizes of the nanoparticles in these "microreactors" are largely controlled by the restricted geometry of the cavities in which nucleation and growth of these particles occur. Thermodynamic and entropic requirements also play a crucial role in determining the size of these clusters.

The layer-by-layer deposition technique of building supramolecular multilayers on solid substrates by adsorbing polyelectrolytes has emerged as a simple means of producing templates of controlled thickness.[12] Extensive works by Decher[12a−d] have established that such multilayers may be reproducibly built and the resultant structure is robust and mechanically and thermally stable. Recently, such films have been utilized in the preparation of electroluminescent devices and zener diodes, and the possibility of their use in flat screen displays has been suggested.[13] In addition to the abovementioned qualities, the porous and supramolecular structure of these films provide opportunities for studying chemical reactions in the nanoscale regime. It has been demonstrated by Stroeve and co-workers[12g−h] that metallic ions can bind to the negatively charged sulfonate groups and the ions can be oxidized to form nanoparticles of these oxides.

In this paper, we report the nucleation and growth of lead sulfide (PbS) nanoparticles in a polydiallyldimethylammonium chloride (PDDA)−polystyrenesulfonate sodium salt (PSS) film produced by the layer-by-layer deposition technique. Although cadmium sulfide (CdS) and cadmium selenide (CdSe) nanoparticles have been extensively examined, few studies on PbS are available, especially in polymers. Interest in PbS arises from the fact that it is a semiconductor having a small band gap (0.41 eV) and large exciton diameter (18 nm) that permits size−quantization effects to be observable even for large particles or crystallites. Moreover, as demonstrated by recent studies, the nonlinear optical (NLO) properties of PbS nanoparticles show large differences in their optical limiting behavior below and above the absorption edge, suggesting that such systems may be utilized in high-speed switching.[13e] While a major thrust in this area of research remains focused on perfecting synthetic techniques to obtain nanoparticles with a narrow particle size distribution, it is worthwhile to investigate in some detail the changes in the optical properties brought about by aggregation of the nanoparticles and correlate them to the size and shape of the particles.

Experimental Section

Lead nitrate $Pb(NO_3)_2$, sodium sulfide (Na_2S), and hydrochloric acid (reagent grade) were purchased from Fisher Chemical Company and used without further purification. PDDA and PSS were products from Polyscience Inc. and were used as received. Deionized water obtained from a Nanopure water purification system (Barnstead) was used for the preparation of all aqueous solutions.

Quartz slides were cleaned with piranha solution, a mixture of concentrated sulfuric acid and hydrogen peroxide in the ratio 7:3 by volume at 80 °C. *Extreme care must be exercised at all times while handling piranha solution as it is extremely corrosive and is known to cause serious damage to skin and tissues.* Treating the quartz slides with piranha removes traces of organic and inorganic impurities sticking to the quartz slides and at the same time makes the surface hydrophilic.

The polymer film, consisting of alternating layers of PDDA and PSS, was built on a quartz substrate by dip coating the substrate into an aqueous solution of PDDA for a period of 20 min, rinsing with water and then drying it completely. The dried film of PDDA was then washed with deionized water and treated with dilute HCl to charge the polymer surface before it was dipped in PSS solution. After keeping the film dipped in PSS for a period of 20 min, the film was rinsed again and completely dried before the process was repeated.[12]

In situ nucleation of PbS particles in the PDDA−PSS film was achieved by first absorbing Pb^{2+} ions into the polymer film by dipping it into an aqueous solution of $Pb(NO_3)_2$ (1 mM) for

(5) (a) Pileni, M. P. *Structure and Reactivity in Reverse Micelles*; Elsevier: Amsterdam, 1989. (b) Lianos, P.; Thomas, J. K. *Chem. Phys. Lett.* **1986**, *125*, 299. (c) Petit, C.; Lixon, P.; Pileni, M. P. *J. Phys. Chem.* **1990**, *94*, 1598. (d) Fendler, J. H. *Chem. Rev.* **1987**, *87*, 877. (e) Watzke, H. J.; Fendler, J. H. *J. Phys. Chem.* **1987**, *91*, 854. (f) Tricot, Y. M.; Emeren, A.; Fendler, J. H. *J. Phys. Chem.* **1985**, *89*, 4721.

(6) (a) Youn, H. C.; Baral, S.; Fendler, J. H. *J. Phys. Chem.* **1998**, *92*, 6320. (b) Kennedy, M. T.; Korgel, B. A.; Montbouquette, H. G.; Zasadinski, J. A. *Chem. Mater.* **1998**, *10*, 2116.

(7) (a) Rajh, T.; Micic, O. I.; Lawless, D.; Serpone, N. *J. Phys. Chem.* **1992**, *96*, 4633. (b) Minti, H.; Eyal, M.; Reisfeld, R.; M. Berkovic, G. *Chem. Phys. Lett.* **1991**, *183*, 277. (c) Rajh, T.; Vuemilovic, M. I.; Dimitrijevic, N. M.; Micic, O. I.; Nozik, A. J. *Chem. Phys. Lett.* **1988**, *143*, 305.

(8) (a) Wang, Y.; Herron, N. *J. Phys. Chem.* **1987**, *91*, 257. (b) Wang, Y.; Herron, N. *J. Phys. Chem.* **1988**, *92*, 4988. (c) Ozin, G. A.; Steele, M. R.; Holmes, A. J. *Chem. Mater.* **1994**, *6*, 999.

(9) (a) Yang, J.; Meldrum, F. C.; Fendler, J. H. *J. Phys. Chem.* **1995**, *99*, 5500. (b) Zhao, X. K.; McCormick, L. D.; Fendler, J. H. *Adv. Mater.* **1992**, *4*, 93. (c) Yang, J.; Fendler, J. H. *J. Phys. Chem.* **1995**, *99*, 5505. (d) Yuan, Y.; Cabasso, I.; Fendler, J. H. *Chem. Mater.* **1990**, *2*, 226.

(10) (a) Wang, Y.; Suna, A.; McHugh, J.; Hilinski, E. F.; Lucas, P. A.; Johnson, R. D. *J. Chem. Phys.* **1987**, *87*, 7315. (b) Wang, Y.; Suna, A.; McHugh, J.; Hilinski, E. F.; Lucas, P. A.; Johnson, R. D. *J. Chem. Phys.* **1990**, *92*, 6927. (c) Wang, Y.; Herron, N.; Mahler, W.; Suna, A. *J. Opt. Soc. Am. B* **1989**, *6*, 808. (d) Wang, Y.; Mahler, W. *Opt. Commun.* **1981**, *61*, 233. (e) Hilinski, E.; Lucas, P.; Wang, Y. *J. Chem. Phys.* **1988**, *89*, 3435. (f) Tassoni, R.; Schrock, R. R. *Chem. Mater.* **1994**, *6*, 744. (g) Sankaran, V.; Cummins, C. C.; Schrock, R. R.; Cohen, R. E.; Silbey, R. J. *J. Am. Chem. Soc.* **1990**, *112*, 6858. (h) Sankaran, V.; Cummins, C. C.; Schrock, R. R.; Cohen, R. E.; Silbey, R. J. *Chem. Mater.* **1993**, *5*, 1133. (i) Kane, R. S.; Cohen, R. E.; Silby, R. J. *Chem. Mater.* **1996**, *8*, 1919.

(11) (a) Murray, C. B.; Norris, D. J.; Bawendi, M. G. *J. Am. Chem. Soc.* **1993**, *115*, 8706. (b) Empedocles, S. A.; Norris, D. J.; Bawendi, M. G. *Phys. Rev. Lett.* **1996**, *77*, 3873.

(12) (a) Decher, G. In *Comprehensive Supramolecular Chemistry*; Sauvage, J. P., Eds.; Pergamon Press: New York, 1996. (b) Decher, G.; Hong, J. D.; Schmitt, J. *Thin Solid Films* **1992**, *210/211*, 831. (c) Decher, G.; Lvov, Y.; Schmitt, J. *Thin Solid Films* **1994**, *244*, 772. (d) Decher, G. *Science* **1997**, 277, 1232. (e) Ferreira, M.; Rubner, M. F. *Macromolecules* **1995**, *28*, 7107. (f) Fou, A. C.; Rubner, M. F. *Macromolecules* **1995**, *28*, 7115. (g) Dante, S.; Hou, Z.; Risbud, S.; Stroeve, P. *Langmuir* **1999**, *15*, 2176. (h) Dutta, A. K.; Jarero, G.; Zhang, L.; Stroeve, P. *Chem. Mat.* **2000**, *12*, 176.

(13) (a) Goldstein, A. N.; Echer, C. M.; Alivisatos, A. P. *Science* **1992**, *256*, 1425. (b) Vossmeyer, T.; Katsikas, L.; Giersig, M.; Popovic, I. G.; Diesner, K.; Chemseddine, A.; Eychmuller, A.; Weller, H. *J. Phys. Chem.* **1994**, *98*, 7665. (c) Fendler, J. H.; Meldrum, F. C. *Adv. Mater.* **1995**, *7*, 607. (d) Dabbousi, B. O.; Murray, C. B.; Rubner, M. F.; Bawendi, M. G. *Chem. Mater.* **1994**, *6*, 216. (e) Colvin, V. L.; Schlamp, M. C.; Alivisatos, A. P. *Nature* **1994**, *370*, 354.

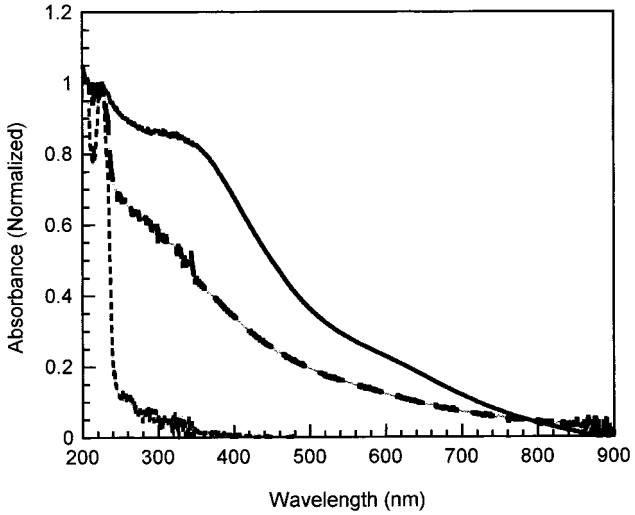

Figure 1. Normalized absorption spectra of PbS particles formed in a 3.5 bilayer thick PDDA−PSS multilayer exposed to 2 (long dashed line) and 10 (continuous line) reaction cycles. The absorption spectra of the pristine PDDA−PSS film is shown by short dashed line.

60 s. Next, the film was rinsed in water for 20 s to remove excess Pb^{2+} from the film surface before exposing it to hydrogen sulfide (H_2S) gas for 5 min to initiate the formation of PbS particles in the film. Finally, the films were rinsed once again in deionized water and dried before the same reaction cycle was repeated.

Absorption spectra of the PbS-loaded films in the 200−900 nm range were recorded on a Cary 13 absorption spectrophotometer. A tungsten lamp was used as the source for examining the 900−350 nm spectral window while a hydrogen lamp was used for the 350−200 nm spectral range.

Transmission electron micrographs of the films were obtained in a conventional manner described in detail elsewhere.[12g−h] Briefly, 3.5 layer pairs of PDDA and PSS were deposited on Formvar-coated, 300 mesh standard copper grids for electron microscopy using the same protocol as used for the quartz slides. These microscopic grids were absorbed with Pb^{2+} by dipping them in an aqueous solution of $Pb(NO_3)_2$ and then exposing them to H_2S gas in a manner identical to that used for preparing the films formed on the quartz substrate. The transmission electron micrographs were recorded on a Hitachi 6010 scanning transmission microscope.

X-ray diffraction pattern of the PDDA−PSS film loaded with PbS particles were recorded on a standard Scintag X-ray diffractometer using the Cu Kα line as the irradiation source. A nickel filter was used to block the Kβ line. All X-ray diffraction data were acquired in the reflection mode with a step size of 0.05°. The diffraction data were stored on a computer and analyzed with software provided by Scintag Inc.

Results and Discussion

Figure 1 shows the UV−visible absorption spectrum of a pristine film of PDDA and PSS that is 3.5 layer pairs thick deposited on a quartz slide (short dashed line). The band at 227 nm corresponds to the absorption band of the PSS molecule, which is confirmed from the absorption spectrum of the PSS and PDDA films taken separately (figure not shown) and discussed in detail elsewhere.[12g−h] Figure 1 also shows the absorption spectra of the same film exposed to 2 and 10 reaction cycles. It may be recalled that each reaction cycle consists of absorbing Pb^{2+} ions in the film by wetting the film in 1 mM $Pb(NO_3)_2$ solution for 60 s, rinsing with water and then exposing it to H_2S gas for 5 min as described in the Experimental Section. Initially, the

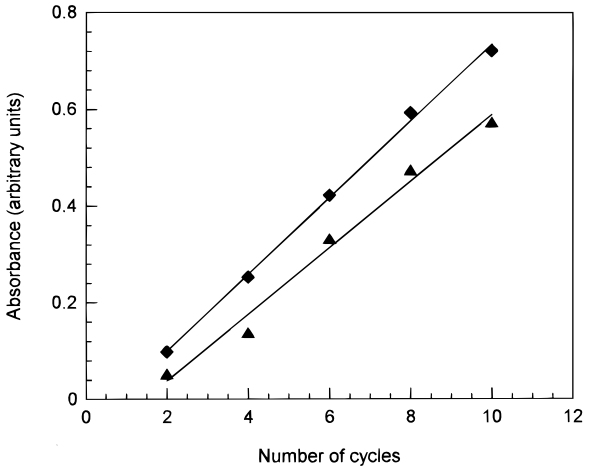

Figure 2. Plot of the absorbance vs the number of reaction cycles. The absorbances were measured at two fixed wavelengths: 430 (squares) and 390 nm (triangles).

Pb^{2+} ions bind to the sulfonate groups in the film, and then, the adsorbed ions react with the H_2S gas to form PbS. Increasing the number of reaction cycles reveal a linear increase in the absorbance of the film, as shown in Figure 2, suggesting an increase in the number density and size of PbS particles formed in the polymer film. Examination of the absorption spectrum in the 200−500 nm spectral window (Figure 1) reveals a shoulder around 300 nm that becomes more pronounced with increasing number of reaction cycles. Similar observations were made by Yang et al.[14] in the absorption spectra of dodecanethiol-capped, PbS nanocrystallites synthesized in the bicontinuous, cubic phase of a lipid and is attributed to the growth of the PbS crystallite size. Inspection of the 450−700 nm region of the absorption spectrum shows a broad hump at 600 nm indicating the possibility of the presence of a weaker absorption band hidden under the tail of an intense band at 300 nm. Deconvolution of the spectral profile (10 cycles, Figure 1) confirms the presence of a broad band in this region with its peak located near 600 nm. The first-order derivatives of the spectra (figure not shown) also exhibited sharp changes in the same region. Although this region of the spectrum has been reported to be featureless by some authors,[14] the presence of an excitonic band at 600 nm has been reported by others.[15] It is observed that this peak at 600 nm shifts to the blue with decreasing number of reaction cycles (Figure 3). These results are consistent with the observation of other workers that increasing size of the aggregates gives rise to a spectral redshift.[15] Additionally, a comparative study of the absorption spectra of the films reveals extensive broadening with an increasing number of reaction cycles. One possible qualitative explanation is that since in the polymer template the shape and sizes of the void spaces vary widely, the crystallites produced through nucleation and growth in such void spaces will alter the size and physical properties. Another plausible explanation is that the strong acid sites on the PSS

(14) Yang, J. P.; Qadri, S. B.; Ratna, B. R. *J. Phys. Chem.* **1996**, *100*, 17225.

(15) (a) Gallardo, S.; Gutierrez, M.; Henglein, A.; Janata, E. *Ber. Bunsen. Ges. Phys. Chem.* **1989**, *93*, 1080. (b) Nenadovic, M. T.; Comor, M. I.; Vasic, V.; Micic, O. I. *J. Phys. Chem.* **1990**, *94*, 6390.

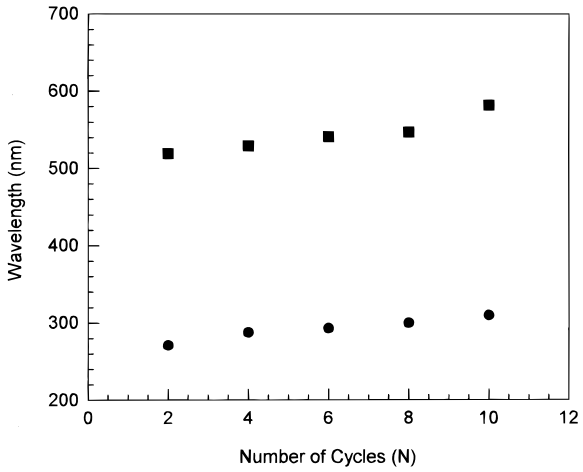

Figure 3. Dependence of the absorption peak position vs the number of reaction cycles to which the films were exposed.

polymer cause Ostwald ripening via the following reaction:

$$PbS + 2H^+ \leftrightarrow Pb^{2+} + H_2S$$

Since the films are not rigorously dried, the presence of water would influence this reaction. Thus, several cycles of PbS/H_2S could give large particles due to Ostwald ripening.

While small particles tend to shift the absorption spectral profile to the blue, larger particles exhibit a redshift. As the absorption spectrum of any section of the film involves an ensemble of particles, the resultant absorption profile is a superposition of the absorption profiles of all the individual particles that is manifested as a broadening of the spectral profile. Increasing the number of the reaction cycles increases the population of the large particles and results in a redshift of the absorption spectral profile which is consistent with our observations and the findings by others.[14,15] Additionally, it must be pointed out that the absorption onset in films exposed to 2 reaction cycles is localized at about 800 nm, and in the film subject to 10 cycles, the onset is about 900 nm whereas in the bulk it is located in the infrared region, with the band gap being 0.41 eV. These results are also consistent with the predictions of the quantum confinement effects and the findings of various authors.[1,2,4] Electron microscopic studies as discussed in a later section do confirm that while small particles are preferentially formed in films subject to a small number of reaction cycles (one or two), large crystallites dominate in films exposed to an increasing number of reaction cycles.

Transmission electron microscopy continues to be a versatile method to examine the composition and structure of microcrystallites down to the nanometer length regime. In an effort to correlate the structure of the crystallites with their optical properties, we have examined in detail the TEM micrographs of films exposed to different number of reaction cycles. Figure 4 corresponds to the micrograph of a film subjected to a single reaction cycle. Examination reveals the presence of large clusters of nanoparticles (<10 nm) in the initial stage of aggregation. A broad distribution in particle sizes exists and is in fact expected; unlike in zeolites or in controlled pore glasses where the pore sizes have a very

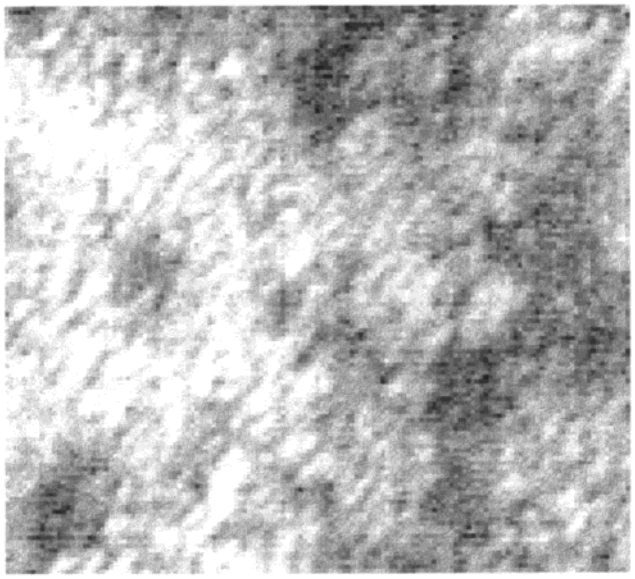

Figure 4. Transmission electron micrograph of a PDDA−PSS film exposed to one reaction cycle. The bar size in the photograph corresponds to 36 nm. The $Pb(NO_3)_2$ concentration was 1 mM.

narrow distribution, here in a polymer matrix the void spaces vary widely. Increasing the number of reaction cycles to two readily reveals an increase in the number density and agglomeration of the particles (Figure 5a). Figure 5b corresponds to the micrograph of the polymer film subject to six reaction cycles. Examination reveals the formation of feathery crystallites. Increasing the number of reaction cycles to eight results in the formation of thick rhomboid structures, as shown in Figure 6a. It is interesting to note that the crystals rapidly grow in length with increasing number of reaction cycles implying that while growth of the crystallites is preferentially facilitated along its long axis, growth in other directions may be physically restricted (Figure 6a,b). This effect could be due to the constrained geometry of the void spaces that are manifested as an increase in the axial ratio of the microcrystals with an increasing number of reaction cycles as evident from Figures 4−6. Similar observations have been reported for FeOOH crystallites.[12h] It must however be pointed out that although the size of particles increase with an increasing number of exposure cycles, a large distribution of particle sizes always exist. Once nucleation is initiated, growth of the crystals proceeds rapidly, resulting in the formation of large crystals. Further, the population density of such crystals is low. In brief, the center of mass of the particle size distribution shifts to larger particle sizes with increasing number of reaction cycles. This phenomenon may be consistent with Ostwald ripening.

Fendler et al.[6,9] have studied in great detail the formation of PbS microcrystals in monolayers of arachidic acid (AA) fabricated at the air−water interface by the Langmuir−Blodgett (LB) technique. TEM studies reveal that oriented equilateral triangular crystallites are formed.[9] These observations are attributed to the formation of an organized template and an excellent match between the crystalline structure of PbS and AA.

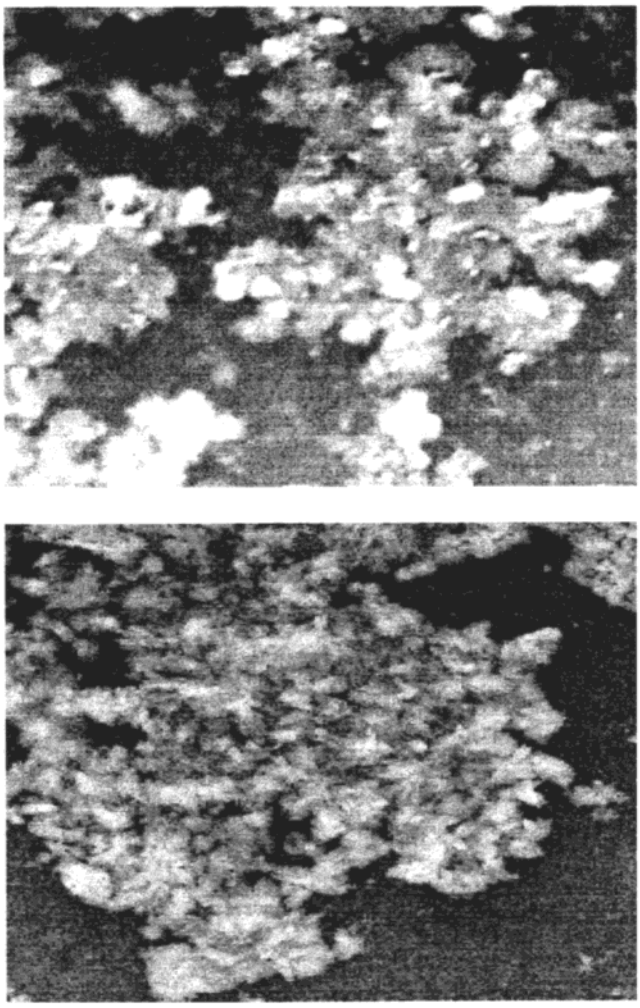

Figure 5. Transmission electron micrograph of a PDDA−PSS film exposed to (a) two and (b) six reaction cycles. The bar size in the photograph corresponds to (a) 97 and (b) 410 nm, respectively. The $Pb(NO_3)_2$ concentration was 1 mM.

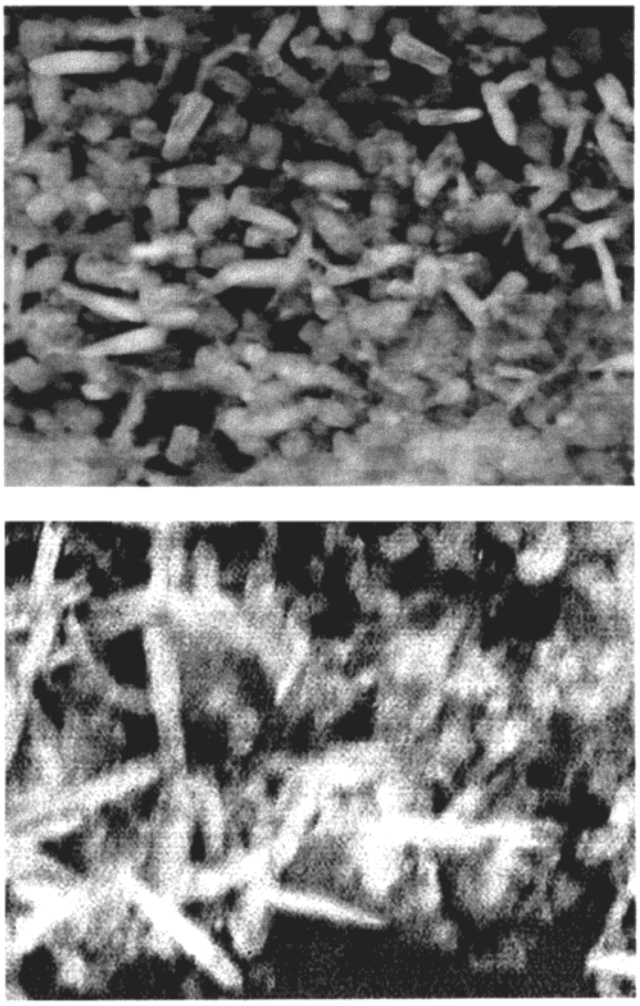

Figure 6. Transmission electron micrograph of a PDDA−PSS film exposed to (a) 8 and (b) 10 reaction cycles. The bar size in the photograph corresponds to (a) 130 and (b) 160 nm. The $Pb(NO_3)_2$ concentration was 1 mM.

Arachidic acid monolayers at the air−water interface form a closely packed hexagonal lattice where the lattice parameter $a = 4.85$ Å. PbS crystals are known to have a typical NaCl structure with a lattice parameter of $a = 5.95$ Å. The Pb−Pb and S−S separation of 4.20 Å corresponding to the (111) face almost perfectly matches the lattice spacing $d(100) = 4.16$ Å for AA that generates equilateral triangular crystals.[9] Altering the organized structure of the AA monolayer by adding octadecylamine (ODA) results in the formation of PbS with different geometries. For instance, when the AA:ODA ratio is 1:1, right-angled triangular crystallites are formed, and when the ratio is AA:ODA is 1:5, nucleation of PbS crystals at the air−water interface ceases. Selected area electron diffraction pattern (SAED) analysis by Fendler et al.[9c] showed that changes in the shape of the crystals originate from crystallization about the (001) basal plane in the 1:1 AA:ODA mixed system in contrast to crystallization about the (111) basal plane in pure AA monolayers. Given the above facts and the lack of any correlation between the structure of PbS and the polymer template, the large differences in the crystal textures obtained by us compared to those obtained by Fendler do not appear to be surprising or unjustified.

Various authors have closely studied the nucleation and growth of PbS particulates in polymer media.[10] Detailed studies have shown that particulates of various different geometries varying from spherical to wormlike configurations may exist.[10f−i] In fact, the size and morphologies may be altered by varying such parameters as temperature, pH, presence of coordinating solvents, nature of the matrix, and time of exposure to H_2S gas.[10i] In an effort to confirm the reliability and reproducibility of our results, we have repeated the studies with a higher concentration of lead nitrate. In this study, a 4 mM concentration of $PbNO_3$ was used in contrast to 1 mM as reported in Figures 4−6. It was found (Figure 7) that the results were similar in that larger crystallites were formed under identical conditions. It is interesting to note that while nanoparticles had started aggregating as demonstrated in Figure 5a, in films subject to two reaction cycles large crystals are already formed (Figure 7a) on increasing the concentration of $PbNO_3$ from 1 to 4 mM.

Since differences in crystal texture may originate from the presence of impurities, we have examined the X-ray diffraction profile obtained for the PDDA−PSS film

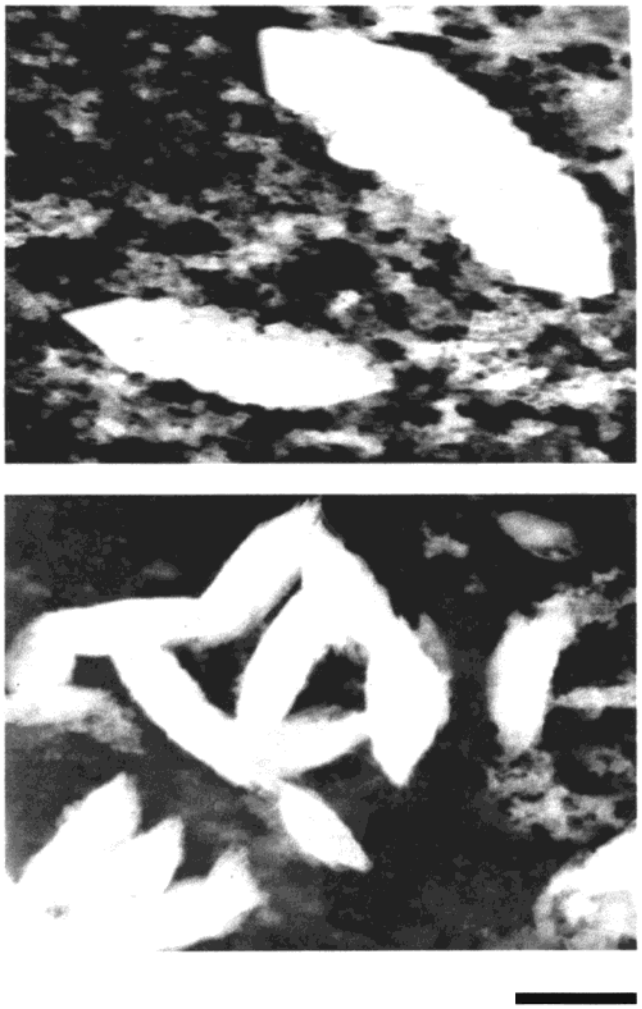

Figure 7. Transmission electron micrograph of a PDDA−PSS film exposed to (a) 2 and (b) 8 reaction cycles. The bar size in the photograph corresponds to (a) 760 and (b) 400 nm. The $Pb(NO_3)_2$ concentration was 4 mM.

loaded with PbS crystallites. It is well-established that such an analysis provides the means of determining not only the crystal texture but also the chemical composition of the materials. Figure 8 shows the X-ray diffraction profile of a PDDA and PSS film (3.5 layer pairs) in which the growth of PbS crystallites has been initiated. Analysis of the band profiles show distinct peaks that are in excellent agreement with the data reported for pure PbS crystals confirming that the film indeed contains PbS crystallites.[16] The broadened profile of the diffraction profile, however, originates from the particulate form of the film. It is well-known (Scherrer formula) that with decreasing particle size, the full-width at half-maximum (fwhm) of the bands increase.[17] We have not attempted to determine the size of the particles because in our system a broad size distribution exists as is evident from TEM studies discussed in an earlier section. Analysis of the diffraction profile and attempts to match the experimental data as a superposition of contributions from PbS and possible impurities such as PbS_2, $PbSO_4$, and $Pb(SO_4)O$ using the

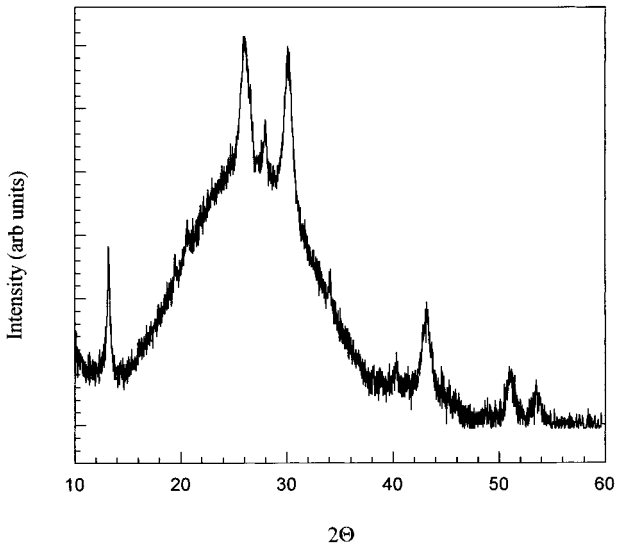

Figure 8. X-ray diffraction profile (intensity vs Θ plot) of PbS crystallites formed in the PDDA−PSS film (20 cycles, $Pb(NO_3)_2$ concentration was 20 mM)

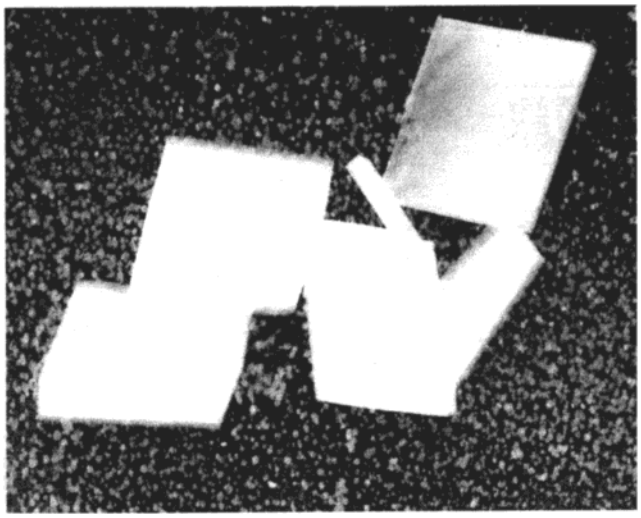

Figure 9. Transmission electron micrograph of a PDDA−PSS film exposed to six reaction cycles in the presence of oxygen. The bar size in the photograph corresponds to 900 nm. The $Pb(NO_3)_2$ concentration was 4 mM.

software elemental analysis program provided by Scintag revealed that although no reasonable matches could be found for PbS_2 and $Pb(SO_4)O$, a small contribution from $PbSO_4$ may however exist. In fact, the weak peak at $2\Theta = 27.96$ may be attributed to the presence of $PbSO_4$. To examine these possibilities further, we have studied the electron micrographs of films prepared in an oxygen-rich environment. The presence of rhombic crystallites (Figure 9) as evident from the image is grossly different from those in Figures 5−7, confirming that these crystallites are morphologically and chemically different from PbS. Indeed, $PbSO_4$ is reported to be rhombic, and the crystal texture is different from that of PbS in that it has a cubic NaCl-type lattice. It must be pointed out that trace amounts of $PbSO_4$ may exist as the preparation of the films were done in a nitrogen-enriched but not completely oxygen-free microenvironment and PbS is known to be oxidized to $PbSO_4$.

(16) *CRC Handbook of Chemistry and Physics*, 73rd ed.; Lide, D. R., Ed.; CRC Press: Boca Raton, FL, 1992.
(17) Cullity, B. D. *Elements of X-ray Diffraction*, 2nd ed.; Addison-Wesley: Reading, MA, 1978.

Conclusions

We have prepared thin polymer films of alternating PDDA and PSS in which PbS nano- and microcrystallites have been formed. The absorption spectral profile of the PbS-loaded polymer film shows a broadening and a redshift in its spectral profile with increasing number of reaction cycles indicating the formation of PbS aggregates. Transmission electron microscopic studies confirm an anisotropic heterogeneous distribution of particles that exhibit a broad distribution in its particle size. While a broad distribution of particle sizes exists at all stages of the crystallization process, the abundance of nanoparticles is apparent in films exposed to a few reaction cycles whereas large particles tend to be formed in films exposed to a large number of reaction cycles. This phenomenon may be consistent with Ostwald ripening.

Acknowledgment. This work was supported in part by the MRSEC program of the National Science Foundation (DMR-g808677).

CM990628C